Physics Letters B 718 (2013) 1321–1333

Contents lists available at SciVerse ScienceDirect

Physics Letters B

www.elsevier.com/locate/physletb

A fresh look into $\overline{m}_{c,b}(\overline{m}_{c,b})$ and precise $f_{D_{(s)},B_{(s)}}$ from heavy–light QCD spectral sum rules ☆

Stephan Narison

Laboratoire Particules et Univers de Montpellier, CNRS-IN2P3, Case 070, Place Eugène Bataillon, 34095 – Montpellier, France

ARTICLE INFO

Article history:
Received 11 September 2012
Received in revised form 13 October 2012
Accepted 22 October 2012
Available online 26 October 2012
Editor: A. Ringwald

Keywords:
QCD spectral sum rules
Meson decay constants
Heavy quark masses

ABSTRACT

Using recent values of the QCD (non-)perturbative parameters given in Table 1 and an estimate of the N3LO QCD perturbative contributions based on the geometric growth of the PT series, we re-use QCD spectral sum rules (QSSR) known to N2LO PT series and including all dimension-six NP condensate contributions in the full QCD theory, for improving the existing estimates of $\overline{m}_{c,b}$ and $f_{D_{(s)},B_{(s)}}$ from the open charm and beauty systems. We especially study the effects of the subtraction point on "different QSSR data" and use (for the first time) the Renormalization Group Invariant (RGI) scale-independent quark masses in the analysis. The estimates [rigourous model-independent upper bounds within the SVZ framework] reported in Table 8: $f_D/f_\pi = 1.56(5)$ [$\leqslant 1.68(1)$], $f_B/f_\pi = 1.58(5)$ [$\leqslant 1.80(3)$] and $f_{D_s}/f_K = 1.58(4)$ [$\leqslant 1.63(1)$], $f_{B_s}/f_K = 1.50(3)$ [$\leqslant 1.61(3.5)$], which improve previous QSSR estimates, are in perfect agreement (in values and precisions) with some of the experimental data on f_{D,D_s} and on recent lattice simulations within dynamical quarks. These remarkable agreements confirm both the success of the QSSR semi-approximate approach based on the OPE in terms of the quark and gluon condensates and of the Minimal Duality Ansatz (MDA) for parametrizing the hadronic spectral function which we have tested from the complete data of the J/ψ and Υ systems. The values of the running quark masses $\overline{m}_c(m_c) = 1286(66)$ MeV and $\overline{m}_b(m_b) = 4236(69)$ MeV from $M_{D,B}$ are in good agreement though less accurate than the ones from recent J/ψ and Υ sum rules.

1. Introduction and a short historical review

The (pseudo)scalar meson decay constants f_P are of prime interests for understanding the realizations of chiral symmetry in QCD. In addition to the well-known values of $f_\pi = 130.4(2)$ MeV and $f_K = 156.1(9)$ MeV [2] which control the light flavor chiral symmetries, it is also desirable to extract the ones of the heavy–light charm and bottom quark systems with high accuracy. These decay constants are normalized through the matrix element:

$$\langle 0|J^P_{\bar{q}Q}(x)|P\rangle = f_P M_P^2, \tag{1}$$

where:

$$J^P_{\bar{q}Q}(x) \equiv (m_q + M_Q)\bar{q}(i\gamma_5)Q, \tag{2}$$

is the local heavy–light pseudoscalar current; $q \equiv d, s$; $Q \equiv c, b$; $P \equiv D_{(s)}, B_{(s)}$ and where f_P is related to the leptonic width:

$$\Gamma(P^+ \to l^+\nu_l) = \frac{G_F^2}{8\pi}|V_{Qq}|^2 f_P^2 m_l^2 M_P \left(1 - \frac{m_l^2}{M_P^2}\right)^2, \tag{3}$$

where m_l is the lepton mass and $|V_{Qq}|$ the CKM mixing angle. Besides some earlier attempts based on non-relativistic potential models to extract these quantities (which are however not applicable for the heavy–light systems), the first bounds on f_D and f_B from QCD spectral sum rules (QSSR) [3][1] were derived by NSV2Z [8], which have been improved four years later in [9–11]. Since then, but long time before the lattice results, different QSSR papers have been published in the literature for estimating $f_{D,B}$.[2] These results look, at first sight, in disagreement among each others and some of them, claimed the observation of the scaling $f_P \sim 1/\sqrt{M_P}$ expected in the large M_P limit [12]. These different papers have been scrutinized in [6,13], where Narison found that the apparent discrepancies between the different results can be solved if one applies carefully the stability criteria (also called sum rule window) of the results versus the external QSSR Laplace/Moments sum rules

☆ Some results of this work have been presented at the 16th QCD International Conference (QCD12), Montpellier, 2–6th July 2012 (Narison, 2012) [1].

E-mail address: snarison@yahoo.fr.

[1] For reviews, see e.g.: [4–7].

[2] For reviews and more complete references, see e.g.: [5,6].

0370-2693
http://dx.doi.org/10.1016/j.physletb.2012.10.057

variables and continuum threshold t_c. In this way, and for given values of $m_{c,b}$, he obtained the values:

$$f_D \simeq (1.31 \pm 0.12) f_\pi, \qquad f_B \simeq (1.6 \pm 0.1) f_\pi, \tag{4}$$

which are independent of the forms of the sum rules used. However, the result has been quite surprising as it indicates a large violation of the heavy quark symmetry scaling predictions,where $1/M_Q$ corrections have been estimated in [14]. This "unexpected result" has been confirmed few years later by lattice calculations [15]. Since then, some progresses have been done for improving the QCD expression of the 2-point correlator. It starts from a confirmation of the SVZ original expression of the LO perturbative and non-perturbative contributions. Then, Broadhurst and Generalis [10,16] have provided the complete PT α_s NLO including light quark mass corrections. It has been completed by the PT α_s^2 N2LO corrections of Chetyrkin and Steinhauser [17] in the case of one heavy and one massless quarks. This result has been completed by the inclusion of the NP contributions up to dimension-six [11] and of the light quark mass corrections to LO by [11,18]. All of these previous QCD expressions have been given in terms of the on-shell quark mass. In [19], Narison has used (for the first time) the running c, b quark masses in the QSSR analysis, by using its known relation with the on-shell mass known at present to NLO [20–22], N2LO [10,16] and N3LO [24] where it has been noticed that the QSSR PT expressions converge faster. It has also been noticed that the values of $f_{D,B}$ are very sensitive to the value of $m_{c,b}$ motivating him to extract $m_{c,b}$ (for the first time) from the known values of M_D and M_B. Recent analysis, including the α_s^2 corrections have been presented in the literature, in the full theory where the running $\overline{\text{MS}}$ mass has been used [25–27] and in HQET [28] where the radiative corrections are large due to the uses of the on-shell mass.[3]

In the following, we shall present analysis based on the full QCD theory where we use as inputs the most recent values of the (non-)perturbative QCD parameters given in Table 1. We assume the geometric growth of the PT series [30] as a dual to the effect of a $1/q^2$ term [31,32] for an estimate of the N3LO perturbative contributions. We shall also study systematically the effect of the substraction points on each "QSSR data" and use (for the first time) in the analysis, the Renormalization Group Invariant (RGI) s, c, b quark masses introduced by [33] and which are scale- and (massless) scheme-independent.

2. QCD spectral sum rules (QSSR)

2.1. The Laplace sum rules (LSR)

We shall be concerned with the two-point correlator:

$$\psi^P_{\bar{q}Q}(q^2) = i \int d^4x e^{iq.x} \langle 0|T J^P_{\bar{q}Q}(x) J^P_{\bar{q}Q}(0)^\dagger|0\rangle, \tag{5}$$

where $J_{\bar{q}Q}(x)$ is the local current defined in Eq. (2). The associated Laplace sum rules (LSR) $\mathcal{L}_{\bar{q}Q}(\tau)$ and its ratio $\mathcal{R}_{\bar{q}Q}(\tau)$ read [3][4]:

$$\mathcal{L}_{\bar{q}Q}(\tau, \mu) = \int_{(m_q+M_Q)^2}^{t_c} dt\, e^{-t\tau} \frac{1}{\pi} \text{Im}\, \psi^P_{\bar{q}Q}(t, \mu), \tag{6}$$

$$\mathcal{R}_{\bar{q}Q}(\tau, \mu) = \frac{\int_{(m_q+M_Q)^2}^{t_c} dt\, t\, e^{-t\tau} \frac{1}{\pi} \text{Im}\, \psi^P_{\bar{q}Q}(t, \mu)}{\int_{(m_q+M_Q)^2}^{t_c} dt\, e^{-t\tau} \frac{1}{\pi} \text{Im}\, \psi_{\bar{q}Q}(t, \mu)}, \tag{7}$$

where μ is the subtraction point which appears in the approximate QCD series when radiative corrections are included. The ratio of sum rules $\mathcal{R}_{\bar{q}Q}(\tau, \mu)$ is useful, as it is equal to the resonance mass squared, in the Minimal Duality Ansatz (MDA) parametrization of the spectral function:

$$\frac{1}{\pi} \text{Im}\, \psi^P_{\bar{q}Q}(t) \simeq f_P^2 M_P^4 \delta(t - M_P^2) + \text{"QCD cont."} \cdot \theta(t - t_c), \tag{8}$$

where f_P is the decay constant defined in Eq. (1) and the higher states contributions are smeared by the "QCD continuum" coming from the discontinuity of the QCD diagrams and starting from a constant threshold t_c.

2.2. The $Q^2 = 0$ moment sum rules (MSR)

We shall also use for the B-meson, the moments obtained after deriving $(n+1)$-times the two-point function and evaluated at $Q^2 = 0$ [3], where an expansion in terms of the on-shell mass M_b can be used. They read:

$$\mathcal{M}^{(n)}_{\bar{q}b}(\mu) = \int_{(m_q+M_b)^2}^{t_c} \frac{dt}{t^{n+2}} \frac{1}{\pi} \text{Im}\, \psi^P_{\bar{q}b}(t, \mu), \tag{9}$$

and the associated ratio:

$$\mathcal{R}^{(n)}_{\bar{q}b}(\mu) = \frac{\int_{(m_q+M_b)^2}^{t_c} \frac{dt}{t^{n+2}} \frac{1}{\pi} \text{Im}\, \psi^P_{\bar{q}b}(t, \mu)}{\int_{(m_q+M_b)^2}^{t_c} \frac{dt}{t^{n+3}} \frac{1}{\pi} \text{Im}\, \psi^P_{\bar{q}b}(t, \mu)}. \tag{10}$$

2.3. Test of the minimal duality ansatz (MDA) from J/ψ and Υ

We have checked explicitly in [6] that the MDA presented in Eq. (8), when applied to the ρ-meson reproduces within 15% accuracy the ratio $\mathcal{R}_{\bar{d}d}$ measured from the total cross-section $e^+e^- \to \text{I} = 1$ hadrons data (Fig. 5.6 of [6]). In the case of charmonium, we have also compared M^2_ψ from $\mathcal{R}^{(n)}_{\bar{c}c}$ with the one from complete data and find a remarkable agreement for higher $n \geqslant 4$ values (Fig. 9.1 of [6]), indicating that for heavy quark systems the rôle of the QCD continuum will be smaller than in the case of light quarks and the exponential weight or high number of derivatives suppresses efficiently the QCD continuum contribution but enhances the one of the lowest ground state in the spectral integral. We redo the test done for charmonium in Fig. 9.1 of [6] and analyze the bottomium channel for the LSR and MSR. We show in Fig. 1(a) the τ-behavior of the ratio of $\mathcal{L}^{\text{exp}}_{\bar{c}c}$ normalized to $\mathcal{L}^{dual}_{\bar{c}c}$ where we have used the simplest QCD continuum expression for massless quarks to order α_s^3 from the threshold t_c[5]:

$$\text{QCD cont.} = 1 + as + 1.5as^2 - 12.07as^3. \tag{11}$$

We show in Fig. 1(b) the τ-behavior of M_ψ, where the continuous (oliva) curve corresponds to $\sqrt{t_c} \simeq M_{\psi(2S)} - 0.15$ GeV. We show a similar analysis for the bottomium sum rules in Fig. 2 for the LSR and in Fig. 3 for the MSR where we have taken $\sqrt{t_c} \simeq M_{\Upsilon(2S)} - 0.15$ GeV. One can see that the MDA, with a value of $\sqrt{t_c}$ around the value of the 1st radial excitation mass, describes quite well the complete data in the region of τ and n where the corresponding sum rules present τ or n stability [35]:

[3] We plan to analyze the HQET sum rules [14,29] in a separate publication.

[4] Radiative corrections to the exponential sum rules have been first derived in [34], where it has been noticed that the PT series has the property of an Inverse Laplace transform.

[5] We have checked that the spectral function including complete mass corrections give the same results.

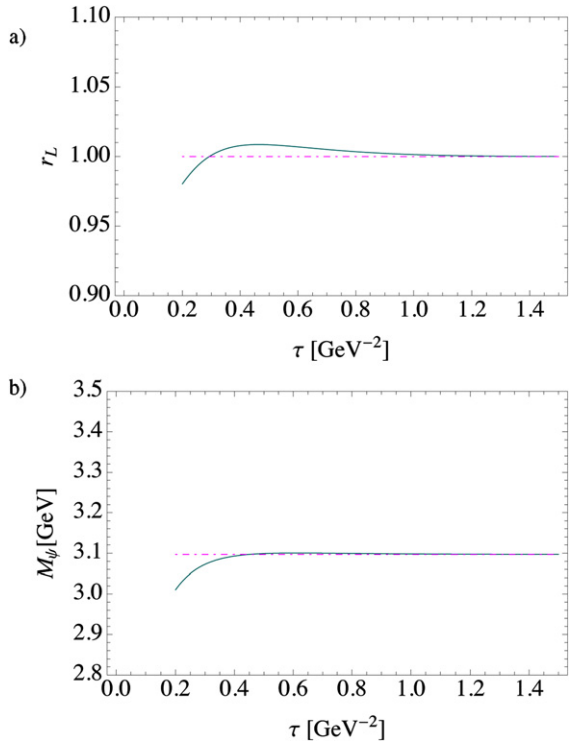

Fig. 1. (a) τ-behavior of the ratio of $\mathcal{L}^{\rm exp}_{\bar{c}c}/\mathcal{L}^{dual}_{\bar{c}c}$ for $\sqrt{t_c} = M_{\psi(2S)} - 0.15$ GeV. The red dashed curve corresponds to the strict equality for all values of τ. (b) The same as (a) but for $M_\psi = \sqrt{\mathcal{R}_{\bar{c}c}}$. (For interpretation of the references to color in this figure, the reader is referred to the web version of this Letter.)

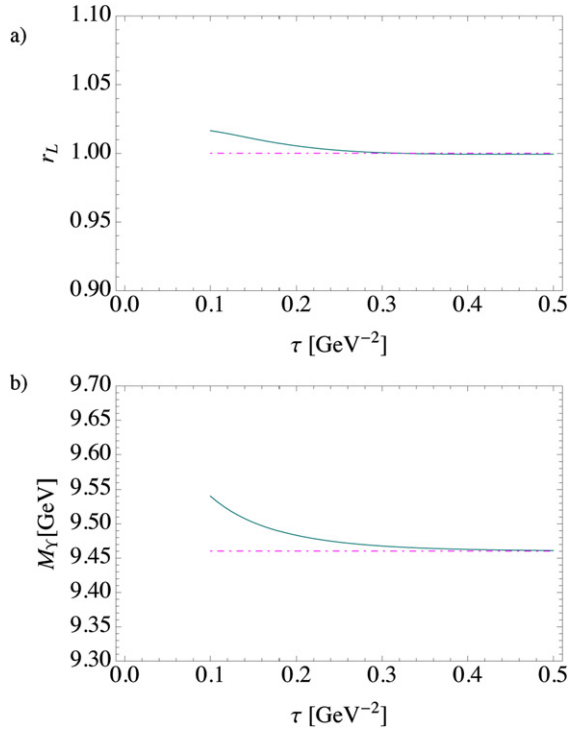

Fig. 2. The same as in Fig. 1 but for the b-quark and for $\sqrt{t_c} = M_{\Upsilon(2S)} - 0.15$ GeV.

$$\tau^\psi \simeq 1.3\text{–}1.4\ \text{GeV}^{-2},$$
$$\tau^\Upsilon \simeq 0.2\text{–}0.4\ \text{GeV}^{-2}, \qquad n^\Upsilon \simeq 5\text{–}7, \tag{12}$$

as we shall see later on. This good description of the data by the MDA shows the efficient rôle of the exponential weight or high

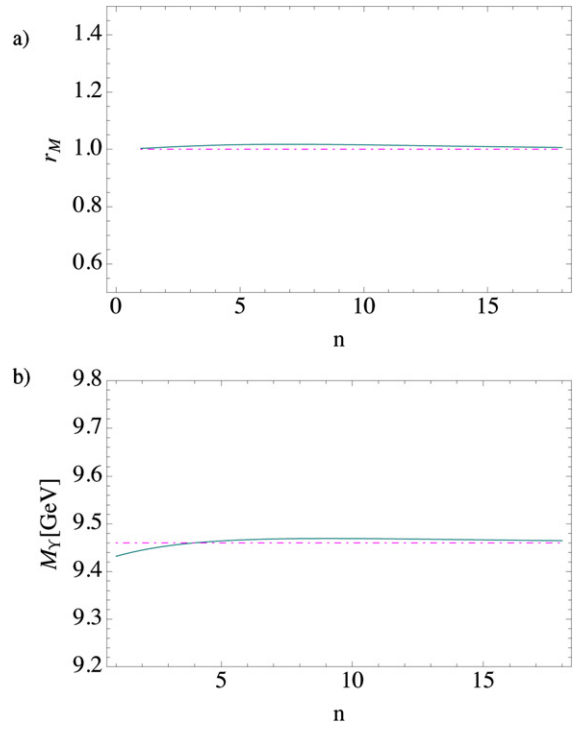

Fig. 3. The same as in Fig. 2 but for the $Q^2 = 0$ moment of the b-quark versus the number of derivatives n.

number of derivatives for suppressing the higher mass states and QCD continuum contribution in the analysis. This nice feature prevents the introduction of some more involved models bringing new parameters in the analysis where some of them cannot be understood from QCD 1st principles. Moreover, MDA has been also used in [36] (called Minimal Hadronic Ansatz in this Letter) in the context of large N_c QCD, where the restriction of an infinite set of large N_c narrow states to a Minimal Hadronic Ansatz which is needed to satisfy the leading short- and long-distance behaves o the relevant Green's functions, provides a very good approximation to the observables one compute.

2.4. Optimal results from stability criteria

Using the theoretical expressions of $\mathcal{L}^{\rm th}_{\bar{d}Q}$ or $\mathcal{M}^{(n)\rm th}_{\bar{d}b}$, and parametrizing its experimental side $\mathcal{L}^{\rm exp}_{\bar{d}Q}$ or $\mathcal{M}^{(n)\,\rm exp}_{\bar{d}b}$ by the MDA in Eq. (8), one can extract the decay constant f_P and the RGI quark mass $\hat{m}_Q$. In principle the equality $\mathcal{L}^{\rm th}_{\bar{d}Q} = \mathcal{L}^{\rm exp}_{\bar{d}Q}$ should be satisfied for any values of the external (unphysical) set of variables (τ, t_c), if one knows exactly $\mathcal{L}^{\rm th}_{\bar{d}Q}$ and $\mathcal{L}^{\rm exp}_{\bar{d}Q}$. Unlike the harmonic oscillator, this is not the case. Using the ratio of moments $\mathcal{R}_{\bar{d}Q}$ for the harmonic oscillator as a function of the imaginary time variable τ, where one knows the exact and approximate results, one can find [37] that the exact energy E_0 of the ground state can be approached from above by the approximate series (see Fig. 4). At the minimum or inflexion point (stability) of the curves, one has a ground state dominance. For small time (large Q^2), all level contributes, while for large time (small Q^2) the series breakdown. We shall apply this stability criterion inspired from quantum mechanics in our analysis.

In principle, the continuum threshold $\sqrt{t_c}$ in Eq. (8) is a free parameter, though one expects its value to be around the mass of the 1st radial excitation because the QCD spectral function is supposed to smear all the higher state contributions in the spectral inte-

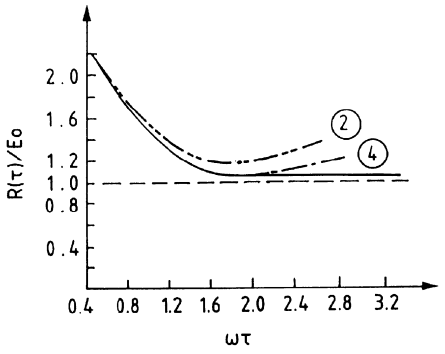

Fig. 4. τ-behavior of $\mathcal{R}(\tau)$ normalized to the ground state energy E_0 for the harmonic oscillator. 2 and 4 indicate the number of terms in the approximate series.

gral as explicitly shown previously in Section 2.3. In order to avoid the model-dependence on the results, Refs. [5,6,13,14,19,25] have considered the conservative range of t_c-values where one starts to have τ- or n-stability until which one reaches a t_c-stability where the contribution of the lowest ground state to the spectral integral completely dominates. For the D and B mesons, this range is [5,6,13,14,19,25]:

$$t_c^D \simeq (5.5 \to 9.5)\ \text{GeV}^2, \qquad t_c^B \simeq (33 \to 45)\ \text{GeV}^2. \tag{13}$$

3. The QCD input parameters

The QCD parameters which shall appear in the following analysis will be the strange, charm and bottom quark masses $m_{s,c,b}$ (we shall neglect the light quark masses $q \equiv u, d$), the light quark condensate $\langle\bar{q}q\rangle$, the gluon condensates $\langle g^2G^2\rangle \equiv \langle g^2 G^a_{\mu\nu} G^{\mu\nu}_a\rangle$ and $\langle g^3G^3\rangle \equiv \langle g^3 f_{abc} G^a_{\mu\nu} G^b_{\nu\rho} G^c_{\rho\mu}\rangle$, the mixed condensate $\langle\bar{q}g\sigma Gq\rangle \equiv \langle\bar{q}g\sigma^{\mu\nu}(\lambda_a/2)G^a_{\mu\nu}q\rangle = M_0^2\langle\bar{q}q\rangle$ and the four-quark condensate $\rho\langle\bar{q}q\rangle^2$, where $\rho \simeq 2$ indicates the deviation from the four-quark vacuum saturation. Their values are given in Table 1 and we shall work with the running light quark parameters known to order α_s^3 [5,6,38]. They read:

$$\begin{aligned}
&\bar{m}_{q,Q}(\tau) = \hat{m}_{q,Q}(-\beta_1 a_s)^{-2/\beta_1} \times C(a_s),\\
&\langle\bar{q}q\rangle(\tau) = -\hat{\mu}_q^3(-\beta_1 a_s)^{2/\beta_1}/C(a_s),\\
&\langle\bar{q}g\sigma Gq\rangle(\tau) = -M_0^2\hat{\mu}_q^3(-\beta_1 a_s)^{1/3\beta_1}/C(a_s),
\end{aligned} \tag{14}$$

where $\beta_1 = -(1/2)(11 - 2n_f/3)$ is the first coefficient of the β function for n_f flavors; $a_s \equiv \alpha_s(\tau)/\pi$; $\hat{m}_{q,Q}$ is the RGI quark mass, $\hat{\mu}_q$ is spontaneous RGI light quark condensate [33]. The QCD correction factor $C(a_s)$ in the previous expressions is numerically:

$$\begin{aligned}
C(a_s) &= 1 + 0.8951a_s + 1.3715a_s^2 + \cdots, \quad n_f = 3,\\
&= 1 + 1.1755a_s + 1.5008a_s^2 + \cdots, \quad n_f = 5,
\end{aligned} \tag{15}$$

which shows a good convergence. We shall use:

$$\alpha_s(M_\tau) = 0.325(8) \quad \Longrightarrow \quad \alpha_s(M_Z) = 0.1192(10) \tag{16}$$

from τ-decays [39,40], which agree perfectly with the world average 2012 [41,42]:

$$\alpha_s(M_Z) = 0.1184(7). \tag{17}$$

We shall also use the value of the running strange quark mass obtained in [43][6] given in Table 1. The value of the running $\langle\bar{q}q\rangle$ condensate is deduced from the value of $(\bar{m}_u + \bar{m}_d)(2) = (7.9 \pm 0.6)$ MeV obtained in [43] and the well-known GMOR relation: $(m_u + m_d)\langle\bar{u}u + \bar{d}d\rangle = -m_\pi^2 f_\pi^2$. The values of the running $\overline{\text{MS}}$ mass $\bar{m}_Q(M_Q)$ recently obtained in Ref. [35] from charmonium and bottomium sum rules, will also be used.[7] Their average is given in Table 1. From which, we deduce the RGI invariant heavy quark masses to order α_s^2, in units of MeV:

$$\hat{m}_c = 1467(14), \qquad \hat{m}_b = 7292(14). \tag{18}$$

For the light quarks, we shall use the value of the RGI mass and spontaneous mass to order α_s for consistency with the known α_s m_s and $\langle\bar{q}q\rangle$ condensate corrections of the two-point correlator. They read, in units of MeV:

$$\hat{m}_s = 128(7), \qquad \hat{\mu}_q = 251(6). \tag{19}$$

Table 1
QCD input parameters.

Parameters	Values	Ref.
$\alpha_s(M_\tau)$	0.325(8)	[39–41]
$\bar{m}_s(2)$	96.1(4.8) MeV	average [43]
$\bar{m}_c(m_c)$	1261(12) MeV	average [35]
$\bar{m}_b(m_b)$	4177(11) MeV	average [35]
$\frac{1}{2}\langle\bar{u}u + \bar{d}d\rangle^{1/3}(2)$	$-(275.7 \pm 6.6)$ MeV	[5,43]
$\langle\bar{s}s\rangle/\langle\bar{d}d\rangle$	0.74(3)	[5,43,47]
M_0^2	(0.8 ± 0.2) GeV^2	[48–50]
$\langle\alpha_s G^2\rangle$	$(7 \pm 1) \times 10^{-2}$ GeV^4	[35,37,39,51–56]
$\langle g^3G^3\rangle$	(8.2 ± 1.0) GeV$^2 \times \langle\alpha_s G^2\rangle$	[35]
$\rho\langle\bar{q}q\rangle^2$	$(4.5 \pm 0.3) \times 10^{-4}$ GeV^6	[39,48,51]

4. QCD expressions of the sum rules

4.1. The LSR

To order α_s^2, the QCD theoretical side of the sum rule reads, in terms of the on-shell heavy quark mass M_Q and for $m_d = 0$:

$$\begin{aligned}
\mathcal{L}_{\bar{d}Q}(\tau) = M_Q^2 \int_{M_Q^2}^{\infty} dt\, e^{-t\tau} \frac{1}{\pi} \text{Im}\,\psi^P_{\bar{q}Q}(t)\Big|_{PT} &+ \frac{\langle\alpha_s G^2\rangle}{12\pi} e^{-z}\\
&- \left\{\left[1 + 2a_s\left[1 + (1-z)\left(\ln\nu^2\tau + \frac{4}{3}\right)\right]\right] e^{-z}\right.\\
&\left. - 2a_s\Gamma(0,z)\right\}\left(\frac{\bar{m}_Q}{M_Q}\right)^2 \bar{m}_Q\langle\bar{d}d\rangle\\
&- \tau e^{-z}\left\{\frac{z}{2}\left(1 - \frac{z}{2}\right) M_Q M_0^2\langle\bar{d}d\rangle\right.\\
&+ \left(2 - \frac{z}{2} - \frac{z^2}{6}\right)\frac{\langle\bar{d}jd\rangle}{6}\\
&- \left(1 + z - 7z^2 + \frac{5}{3}z^3\right)\frac{\langle g^3G^3\rangle}{2880\pi^2}\\
&\left. + \left[5\tilde{L}(12 - 3z - z^2)z - 9 + 11z + \frac{41}{2}z^2\right.\right.\\
&\left.\left. + \frac{5}{2}z^3\right]\frac{\langle j^2\rangle}{2160\pi^2}\right\},
\end{aligned} \tag{20}$$

where:

[6] This value agrees and improves previous sum rules results [44].

[7] These values agree and improve previous sum rules results [3–6,45,46].

$$\text{Im}\,\psi^P_{\bar{q}Q}(t)\big|_{PT} = \frac{1}{8\pi^2}\left[3t(1-x)^2\left(1+\frac{4}{3}a_s f(x)\right)+a_s^2 R_{2s}\right] \quad (21)$$

with: $z \equiv M_Q^2\,\tau$; $x \equiv M_Q^2/t$; $a_s \equiv \alpha_s/\pi$; $\tilde{L} \equiv \ln(\mu M_Q\,\tau) + \gamma_E$: $\gamma_E = 0.577215\ldots$; μ is an arbitrary subtraction point; R_{2s} is the α_s^2-term obtained semi-analytically in [17] and is available as a Mathematica package program Rvs.m. Neglecting m_d, the PT NLO terms read [10]:

$$\begin{aligned} f(x) = {} & \frac{9}{4} + 2\,\text{Li}_2(x) + \log x \log(1-x) \\ & - \frac{3}{2}\log(1/x-1) - \log(1-x) \\ & + x\log(1/x-1) - \big(x/(1-x)\big)\log x. \end{aligned} \quad (22)$$

The contribution up to the $d=4$ gluon condensate and up to $d=6$ quark condensates have been obtained originally by NSV2Z [8]. The contribution of the $d=6$ $\langle g^3 f_{abc} G^3\rangle$ and $\langle j^2\rangle$ gluon condensates have been deduced from the expressions given by [11] (Eqs. II.4.28 and Table II.8) where:

$$\begin{aligned} \langle \bar{d}jd\rangle &\equiv \left\langle \bar{d} g\gamma_\mu D^\mu G_{\mu\nu}\frac{\lambda_a}{2} d\right\rangle = g^2\left\langle \bar{d}\gamma_\mu\frac{\lambda_a}{2} d\sum_q \bar{q}\gamma_\mu\frac{\lambda_a}{2} q\right\rangle \\ &\simeq -\frac{16}{9}(\pi\alpha_s)\rho\langle\bar{d}d\rangle^2, \\ \langle j^2\rangle &\equiv g^2\langle (D_\mu G^a_{\nu\mu})^2\rangle = g^4\left\langle\left(\sum_q \bar{q}\gamma_\nu\frac{\lambda^a}{2} q\right)^2\right\rangle \\ &\simeq -\frac{64}{3}(\pi\alpha_s)^2\rho\langle\bar{d}d\rangle^2, \end{aligned} \quad (23)$$

after the use of the equation of motion. $\rho \simeq (2\pm 0.2)$ measures the deviation from the vacuum saturation estimate of the $d=6$ quark condensates [39,48,51].

The α_s correction to $\langle\bar{d}d\rangle$, in the $\overline{\text{MS}}$-scheme, comes from [26], where the running heavy quark mass $\overline{m}_Q$ enters into this expression. Using the known relation between the running $\bar{m}_Q(\mu)$ and on-shell mass M_Q in the $\overline{\text{MS}}$-scheme to order α_s^2 [20–24]:

$$\begin{aligned} M_Q = \overline{m}_Q(\mu)\Bigg[& 1 + \frac{4}{3}a_s + (16.2163 - 1.0414 n_l)a_s^2 \\ & + \ln\left(\frac{\mu}{M_Q}\right)^2\left(a_s + (8.8472 - 0.3611 n_l)a_s^2\right) \\ & + \ln^2\left(\frac{\mu}{M_Q}\right)^2 (1.7917 - 0.0833 n_l)a_s^2 + \cdots\Bigg], \end{aligned} \quad (24)$$

for n_l light flavors, one can express all terms of the previous sum rules with the running mass $\overline{m}_Q(\mu)$. It is clear that, for some non-perturbative terms which are known to leading order of perturbation theory, one can use either the running or the pole mass. However, we shall see that this distinction does not affect, in a visible way, the present result, within the accuracy of our estimate, as the non-perturbative contributions are relatively small though vital in the analysis.

4.2. The MSR

The moments read for $m_d = 0$:

$$\mathcal{M}^{(n)}_{\bar{d}b} = \int_{M_b^2}^{t_c} \frac{dt}{t^{n+2}}\frac{1}{\pi}\,\text{Im}\,\psi^B_{\bar{d}b}(t)\Big|_{PT}$$

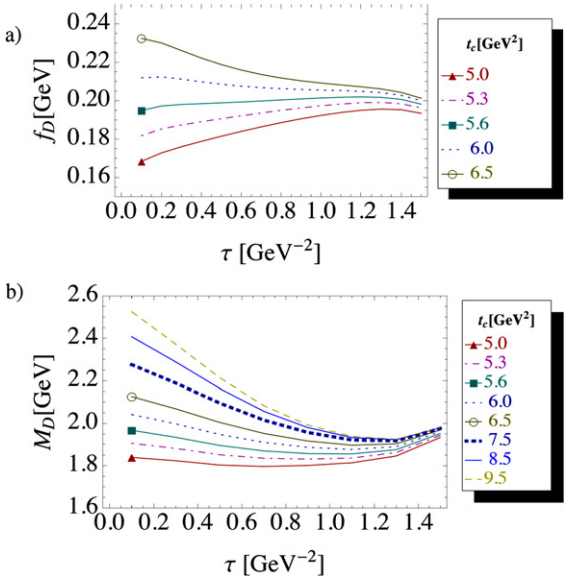

Fig. 5. (a) τ-behavior of f_D from $\mathcal{L}_{\bar{d}c}$ for different values of t_c, for a given value of the subtraction point $\mu = \tau^{-1/2}$ and for $\hat{m}_c = 1467$ MeV as given in Eq. (18); (b) the same as (a) but for M_D from $\mathcal{R}_{\bar{d}c}$.

$$\begin{aligned} & + \frac{1}{(M_b^2)^{n+1}}\Bigg\{-M_b\langle\bar{d}d\rangle + \frac{\langle\alpha_s G^2\rangle}{12\pi} \\ & + (n+1)(n+2)\frac{1}{4M_b}M_0^2\langle\bar{d}d\rangle \\ & - (n+1)(n+2)(n+9)\frac{1}{M_b^2}\frac{\langle\bar{d}jd\rangle}{36} \\ & - (n+3)\big(5n^2+9n+1\big)\frac{1}{3M_b^2}\frac{\langle g^3G^3\rangle}{2880\pi^2} \\ & - \Bigg\{\frac{1}{3}\big(20n^3+186n^2+337n+117\big) \\ & - 5(n+2)\Bigg[S_4\big(n^2+7n+12\big) + 3S_3(n+3) - 12S_2 \\ & - \big(n^2+10n+9\big)\ln\left(\frac{M_b}{\mu}\right)\Bigg]\Bigg\}\frac{1}{M_b^2}\frac{\langle j^2\rangle}{2160\pi^2}\Bigg\}, \end{aligned} \quad (25)$$

where:

$$S_p \equiv \sum_{i=0}^{n}\frac{1}{i+p}. \quad (26)$$

5. Estimates of f_P and $\hat{m}_Q$ at $\mu = \tau^{-1/2}$ from LSR

After inspection, one finds that f_P and the RGI mass $\hat{m}_Q$ can only be simultaneously determined from $\mathcal{L}_{\bar{d}Q}(\tau,\mu)$ and $\mathcal{R}_{\bar{d}Q}(\tau,\mu)$ evaluated at $\mu = \tau^{-1/2}$. For other values of μ, only $\mathcal{L}_{\bar{d}c}(\tau,\mu)$ present τ stability at reasonable values of $\tau \leqslant 1.2\,\text{GeV}^{-2}$, which is not $\mathcal{R}_{\bar{d}c}(\tau,\mu)$. This particular value of $\mu = \tau^{-1/2}$ is also interesting because the subtraction scale moves with the sum rule variable τ in the analysis.

5.1. Analysis of the τ-and t_c-stabilities of $\mathcal{L}_{\bar{d}c}$ and $\mathcal{R}_{\bar{d}c}$

Using the central values of the QCD input parameters in Table 1 and in Eqs. (16), (18) and (19), one can show in Fig. 5 the influences of τ and t_c on the value of f_D and M_D for a given value of

the subtraction point $\mu = \tau^{-1/2}$, where, the τ-stability for f_D is reached for:

$$\tau_0^D \simeq (0.8\sim 1.2)\ \text{GeV}^{-2}, \qquad t_c^D \simeq (5.3 \to 6.5)\ \text{GeV}^2. \tag{27}$$

When extracting the RGI mass $\hat{m}_c$ from $\mathcal{R}_{\bar{d}c}$ by requiring that it reproduces the experimental mass squared M_D^2, one can notice in Fig. 5 that, unlike f_D, M_D present τ-stability for larger range of t_c-values:

$$t_c^D \simeq (5.3 \to 9.5)\ \text{GeV}^2. \tag{28}$$

The existence of τ-stability at values of t_c below 5.3 GeV^2 depends on the heavy quark mass value and disappears when we require the sum rule to reproduce the value of M_D, such that we shall not consider a such region. The values of $t_c \simeq (6.5 \sim 9.5)$ GeV^2 given in Eqs. (27) and (28) correspond the beginning of t_c stability, where at the extremal values $\tau \simeq (1.2 \sim 1.3)$ GeV^{-2}, optimal results for f_D, M_D can be extracted (principle of minimal sensitivity on external variable) and where there is a balance between the continuum (left) and non-perturbative (right) contributions (see also similar cases of the harmonic oscillator in Fig. 4 and of the Laplace sum rules for charmonium and bottomium in [35,37]). Like in earlier versions of this work [13,14,19,25], we consider this large range of t_c-values in the aim to extract the most conservative result from the analysis and to avoid, in the same way, any (ad hoc) external input for fixing the exact value of t_c. This procedure implies a larger error in our result than often quoted in the literature where (to my personal opinion) the systematics have been underestimated. A similar procedure will be done in the following and for the B-meson channel.

5.2. Analysis of the convergence of the QCD series

We study the convergence of the QCD series in the case of the charm quark at a such low value of the subtraction point $\mu = \tau^{-1/2}$ and taking $t_c = 6$ GeV^2. We work in the $\overline{\text{MS}}$-scheme as we know from previous works [19] that the PT series converge better than using the on-shell subtraction. In so doing, we estimate the α_s^3 N3LO contribution using a geometric PT series as advocated in [30] which is dual to the effect of the $1/q^2$ term when large order PT series are resummed. We show the τ-behavior of f_D in Fig. 6. One can notice that, all corrections act in a positive way. The prediction increases by about 17% from LO to NLO and another 14% from NLO to N2LO but remains unaffected by the inclusion of the N3LO contribution estimated above. These features indicate that the PT series converge quite well at this low scale, while the size of each PT corrections are reasonably small and will be even smaller for higher values of the subtraction point μ and for the B-meson. Therefore, a confirmation of this N3LO estimate requires an explicit evaluation of this contribution.

As far as the non-perturbative contributions are concerned, their effects are relatively small.

5.3. QCD and systematic error estimates

Using the previous QCD input parameters and their corresponding errors, we deduce the different errors on f_P and $\hat{m}_Q$ given in Table 2, where the optimal results have been taken at the τ- and t_c-stability regions mentioned in the previous subsection:

$$\tau^D \simeq 0.8\text{–}1.3\ \text{GeV}^{-2}, \qquad t_c^D \simeq (5.3 \to 6.5\text{–}9.5)\ \text{GeV}^2. \tag{29}$$

As mentioned earlier, we consider a such large range of t_c-values in the aim to extract the most conservative result from the analysis. However, this procedure induces a larger error in the analysis

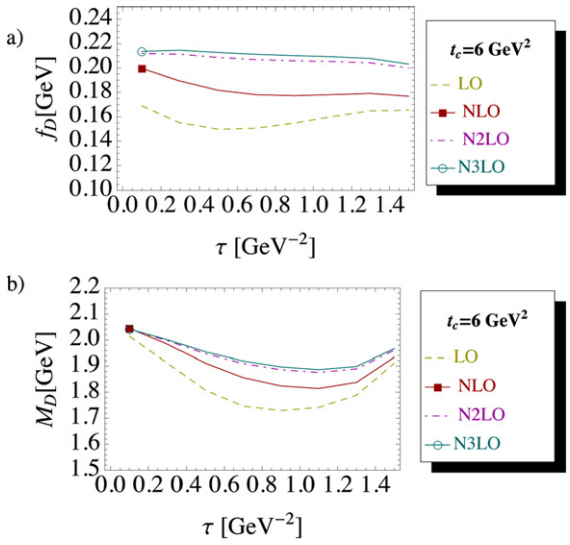

Fig. 6. τ-behavior of f_D from LSR for $t_c^D = 6$ GeV^2, for $\hat{m}_c = 1467$ MeV, for a given value of the subtraction point $\mu = \tau^{-1/2}$ GeV and for different truncations of the QCD PT series, where the estimated N3LO contribution is small indicating a good convergence of the series; (b) the same as (a) but for M_B.

than the one quoted in the literature using some other models or using some other criteria. In fact, the range of values of our result includes most of the predictions given in the literature which are often quoted with smaller errors. Therefore, we expect that, within this procedure, we take properly into account most of the systematics of the sum rule approach.

In so doing, we take the central value of f_D in Table 2 as coming from an arithmetic average of its values from the different t_c given in the legend of Fig. 5 inside the range given by Eq. (27). We may have improved the accuracy of our predictions by introducing more model-dependent new parameters for parametrizing the continuum contribution, which we would not do as, in addition to the test performed in Section 2.3, we also want to check the degree of accuracy of the MDA parametrization for the heavy–light systems by confronting the results obtained in this Letter with the some known data on f_P or from lattice simulations. Indeed, such tests are important as the MDA model is widely used in the literature for predicting some not yet measured masses of new exotic hadrons like four-quark, molecules [57] and hybrid [58] states. However, we do not also try to fix more precisely t_c by e.g. using Finite Energy Sum Rule [53] like did the authors in Ref. [59] as we want to have more conservative results.

5.4. Results for f_D and $\hat{m}_c$

Considering the common range of t_c-values for f_D and M_D given in Eq. (27), we obtain the results quoted in Table 2 which come from an arithmetic average of optimal values obtained at different t_c values in Eq. (27)[8]:

$$f_D = 204(11)\ \text{MeV},$$
$$\hat{m}_c = 1490(77) \quad \Longrightarrow \quad \overline{m}_c(\overline{m}_c) = 1286(66)\ \text{MeV}, \tag{30}$$

which we consider as improvement of the result obtained from the same sum rule and at the same subtraction point by [19][9]:

[8] Using the larger range of t_c-values, we would have obtained a slightly different value: $\hat{m}_c \simeq 1492(102)_{t_c}(82)_{qcd}$ MeV, where the errors come respectively from the choice of t_c and QCD parameters given in details in Table 2.

[9] An extended discussion about the value of f_D at different subtraction points will be done in the next section.

Table 2
Central values and corresponding errors for f_P and $\hat{m}_Q$ in units of MeV from the LSR at the subtraction point $\mu = \tau^{-1/2}$. We have used $\hat{m}_Q$ in Eq. (18) for getting f_P. The $+$ (resp. $-$) sign means that the values of f_P, $\hat{m}_Q$ increase (resp. decrease) when the input increases (resp. decreases). The relative change of sign from c to b in some errors is due to the effects of τm_Q^2 appearing the OPE. Notice that the error in $\langle G^2\rangle$ also affects the $\langle G^3\rangle$ contribution. The total error comes from a quadratic sum.

	Value	t_c	α_s	α_s^3	m_Q	$\langle\bar{d}d\rangle$	$\langle G^2\rangle$	M_0^2	$\langle\bar{d}d\rangle^2$	$\langle G^3\rangle$	Total
f_D	204	+4	−9	+3	−2	+3.5	+0.5	−0.5	−0.01	+0.03	11
f_B	201	+7	−10	+1	−2	+1.9	+0.05	−0.25	−0.00	+0.00	13
$\hat{m}_c$	1457	−44	−64	−24	0	+22	+5	−38	+1.5	−0.8	93
$\hat{m}_b$	7272	−150	−114	−14	0	+20	+5	−39	−13	−14	195

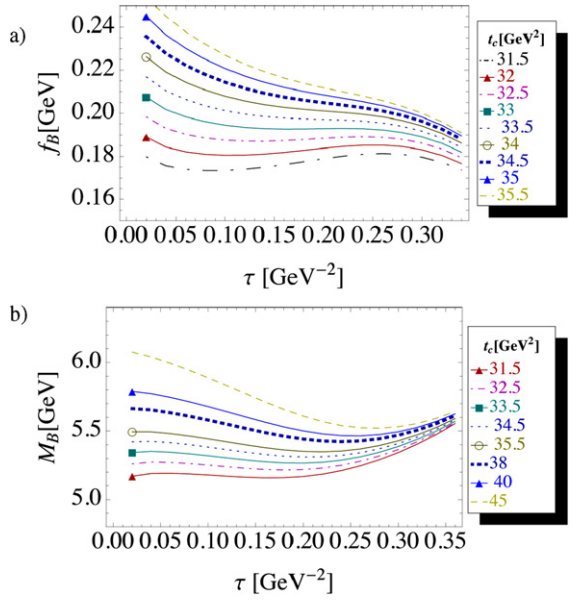

Fig. 7. (a) τ-behavior of f_B from $\mathcal{L}_{\bar{d}b}$ for different values of t_c, for a given value of the subtraction point $\mu = \tau^{-1/2}$ and for $\hat{m}_b = 7292$ MeV as given in Eq. (18); (b) the same as (a) but for M_B from $\mathcal{R}_{\bar{d}b}$.

$$f_D = 205(20)\ \text{MeV}, \qquad \overline{m}_c(\overline{m}_c) = 1100(40)\ \text{MeV}. \tag{31}$$

The smaller errors in the present analysis, come from more precise input parameters, more complete NP-corrections included into the OPE and more constrained range of t_c-values.The value obtained in Eq. (30) also agrees within errors with the accurate determination from charmonium systems quoted in Table 1 though less accurate. The main sources of errors from the present determination can be found in Table 2. One can notice that the contributions of the $d = 6$ condensates are negligible for f_D (less than 0.3 MeV) and small for m_c ($\langle\bar{d}d\rangle^2$ and $\langle G^3\rangle$ which contribute respectively to 17 and 6 MeV).

5.5. Extension of the analysis to f_B and $\hat{m}_b$

We extend the previous analysis to the case of the b-quark. We show in Fig. 7 the τ-behaves of f_B and M_B for different values of t_c. One can see, that in this channel, τ-stability for f_B is reached at [10]:

$$\tau_0^B \simeq (0.2 \sim 0.26)\ \text{GeV}^{-2}, \qquad t_c^B \simeq (33 \to 35)\ \text{GeV}^2, \tag{32}$$

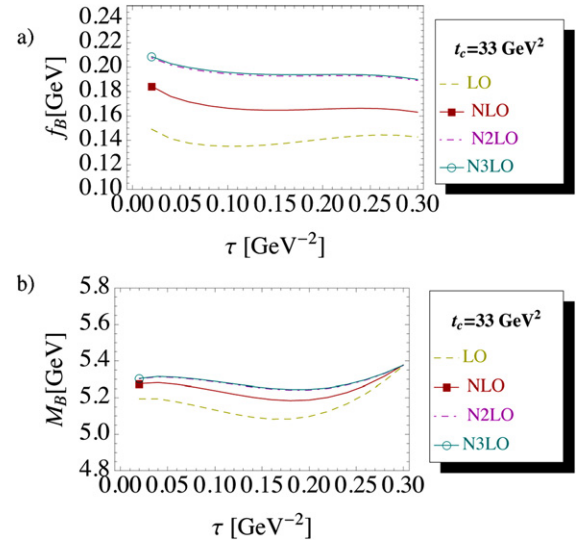

Fig. 8. τ-behavior of f_B from LSR for $t_c^B = 33$ GeV^2, for $\hat{m}_b = 7292$ MeV, for a given value of the subtraction point $\mu = \tau^{-1/2}$ GeV and for different truncations of the QCD PT series; (b) the same as (a) but for M_B.

while, like in the case of M_D, M_B stabilizes for a larger range of values[11]:

$$t_c^B \simeq (33 \to 45)\ \text{GeV}^2. \tag{33}$$

We show in Fig. 8 the predicted values of f_B and M_B for a given value of $\hat{m}_b$ and for different truncations of the PT QCD series. Using the same procedure as in the charm quark case and considering the range of t_c in Eq. (32), where the central values of f_B and $\hat{m}_b$, in units of MeV in Table 2 comes from an arithmetic average of different optimal values in the range of t_c in Eq. (32), we deduce the estimate in units of MeV:

$$f_B = 201(13),$$
$$\hat{m}_b = 7272(195) \quad \Longrightarrow \quad \overline{m}_b(\overline{m}_b) = 4164(112), \tag{34}$$

which we again consider as improvement of the result from [19]:

$$f_B = 203(23)\ \text{MeV}, \qquad \overline{m}_b(\overline{m}_b) = 4050(60)\ \text{MeV}, \tag{35}$$

obtained from the same sum rule.

6. Effects of the subtraction point on $f_{D,B}$ from LSR

The choice of subtraction points is also one large source of errors and discrepancies in the existing literature. In order to cure these weak points, we extract the values of $f_{D,B}$ and the corresponding errors at a given value of the subtraction point μ. We

[10] The apparent minima at $\tau \leqslant 0.1$ GeV^2 obtained for lower values of tc corresponds to the region where the continuum contribution to the spectral integral is dominant and should not be considered.

[11] Like in the case of the charm quark, we shall not consider values of $t_c \leqslant 32.5$ GeV^2 where the τ-stability disappears, when one requires the sum rule to reproduce M_B.

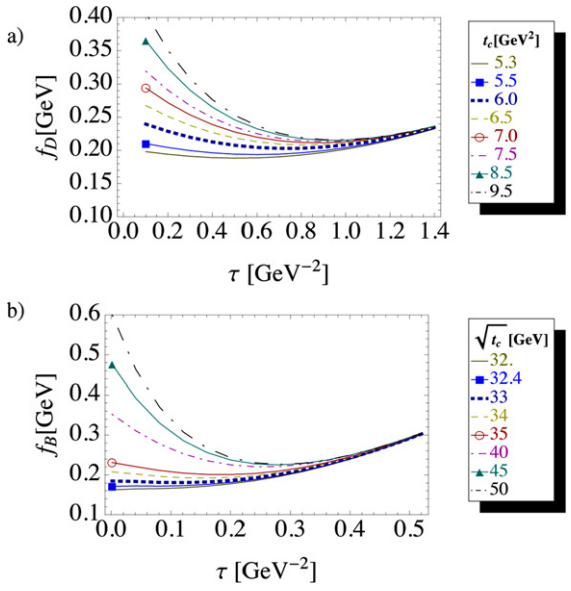

Fig. 9. (a) τ-behavior of f_D from LSR for different values of t_c, for a given value of the subtraction point $\mu = 1.4$ GeV and for $\hat{m}_c = 1467$ MeV; (b) the same as (a) but for f_B, using $\mu = 3$ GeV and $\hat{m}_b = 7292$ MeV.

show in Fig. 9 the τ-behavior of $f_{D,B}$ for given values of μ and $\hat{m}_{c,b}$. We show in Tables 3 and 4, the results of the analysis including the different sources of the errors, where the typical sizes normalized to the values of $f_{D,B}$ are:

- f_D: (7–8)% from t_c, (0.7–2)% from the PT contributions, 0.5% from m_c and (0.9–1.6)% from the NP-contributions.
- f_B are: (2–4)% from t_c, 4% from the PT contributions, 4% from m_b and (0.8–1.5)% from the NP-contributions.

We show in Figs. 10 and 14, the set of "QSSR data points" obtained in this way for different values of μ.

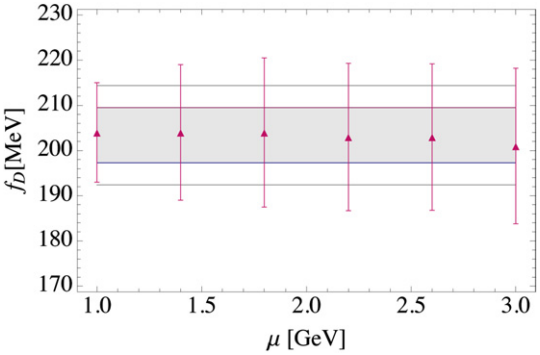

Fig. 10. Values of f_D from LSR at different values of the subtraction point μ and for $\hat{m}_c = 1467$ MeV. The filled (grey) region is the average with the corresponding averaged errors. The dashed horizontal lines are the values if one takes the errors from the best determination.

6.1. Final results for f_D and f_B from LSR

Using the fact that the "physical observable" is independent of μ, we average (fit horizontally) the different data points of f_D from LSR in Tables 2 and 3 and Fig. 10 (red triangle). The average is represented by the horizontal band in Fig. 10. The narrower (grey) domain corresponds to the resulting averaged error, while the larger one corresponds to the case where the error from the most precise determination has been taken. A similar analysis for f_B from LSR has been done using the data in Tables 2 and 4 and Fig. 14. We deduce from this analysis, the final results:

$$f_D = 204(6)\ \text{MeV} \equiv 1.56(5) f_\pi,$$
$$f_B|_{\text{LSR}} = 207(8)\ \text{MeV} \equiv 1.59(6) f_\pi, \tag{36}$$

where the quoted errors are the averaged errors. The previous errors are multiplied by about 1.8 for f_D and 1.65 for f_B if one keeps the errors from the most precise determinations.

Table 3
Central values and corresponding errors for f_D in units of MeV from the LSR at different values of the subtraction point μ in units of MeV and for $\hat{m}_c = 1467$ MeV. The + (resp. −) sign means that the values of f_D increase (resp. decrease) when the input increases (resp. decreases). The total error comes from a quadratic sum.

μ	f_D	t_c	α_s	α_s^3	m_c	$\langle\bar{d}d\rangle$	$\langle G^2\rangle$	M_0^2	$\langle\bar{d}d\rangle^2$	$\langle G^3\rangle$	Total
1.4	204	+14	−1.3	+4	−1	+3	+1	+0.6	+0.6	+0.6	15.0
1.8	204	+16	−1.2	+2.7	−0.9	+2.3	+0.3	+0.4	0.0	0.0	16.5
2.2	203	+16	−1.0	+2.2	−0.7	+2.1	+0.3	+0.3	0.0	0.0	16.3
2.6	203	+16	−1.1	+1.5	−1.1	+1.6	+0.3	0.0	−0.6	−0.5	16.2
3.0	201	+17	−0.8	+1.2	−0.8	+1.6	+0.3	+0.1	−0.5	−0.5	17.2

Table 4
Central values and corresponding errors for f_B in units of MeV from the LSR and MSR at different values of the subtraction point μ in units of GeV for $\hat{m}_b = 7292$ MeV. The + (resp. −) sign means that the values of f_B increase (resp. decrease) when the input increases (resp. decreases). The total error comes from a quadratic sum.

μ	f_B	t_c	α_s	α_s^3	m_b	$\langle\bar{d}d\rangle$	$\langle G^2\rangle$	M_0^2	$\langle\bar{d}d\rangle^2$	$\langle G^3\rangle$	Total
LSR											
3	196	+22	−8.0	−1.6	−1.1	+1.9	+0.1	+0.4	0.0	0.0	23.6
4	210	+23	−7.6	−0.3	−1.2	+1.7	+0.1	−0.2	0.0	0.0	24.3
5	213	+24	−7.6	+0.4	−1.2	+1.5	+0.1	0.0	0.0	0.0	25.3
6	217	+24	−7.3	+0.1	−1.2	+1.6	+0.1	0.0	0.0	0.0	25.2
7	218	+21	−7.1	+0.5	−1.0	+1.5	+0.1	0.0	0.0	0.0	22.3
MSR											
3	183	+7	−16	0	−2.5	+2	0	−5	0	0	18.4
4	199	+10	−22	0	−3	+3	0	−9	0	0	26.1
5	216	+11	−19	+1	−3	+4	0	−13	0	0	26.0
6	227	+17	−21	0	−4	+3	0	−17	0	0	32.3
7	235	+20	−21	+0.5	−3	+4	0	−20	0	0	35.6

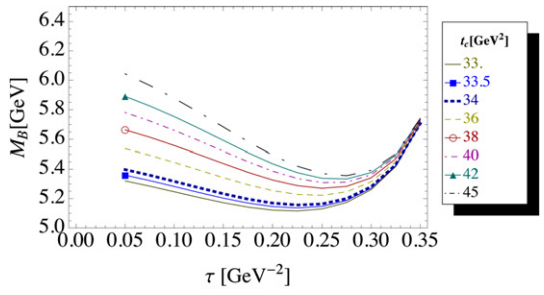

Fig. 11. τ behavior of M_B from LSR for different values of t_c, for $\hat{m}_b = 7292$ MeV and at the subtraction point $\mu = M_b$.

6.2. Final value of $\hat{m}_b$ from LSR

In addition to the sum rule $\mathcal{R}_{\bar{d}b}$ subtracted at $\mu = \tau^{-1/2}$, we also notice that the sum rule $\mathcal{R}_{\bar{d}b}$ subtracted at $\mu = M_b$, where the $\log(\mu/M_b)$-term disappears in the QCD expression, presents τ-stability [see Fig. 11] and can then provide another estimate of $\hat{m}_b$. The result is given in Table 5. Taking the average of this result with the previous one in Table 2, we deduce in units of MeV:

$$\hat{m}_b|_{\rm LSR} = 7326(178) \quad \Longrightarrow \quad \overline{m}_b(\overline{m}_b)|_{\rm LSR} = 4195(102), \tag{37}$$

7. $Q^2 = 0$ moment sum rules (MSR) for the B meson

7.1. Convergence of the PT series

We show in Fig. 12 the n-behaves of f_B and M_B for different values of t_c, where one can realize a good convergence when the N3LO term is included.The convergence of the PT series is comparable with the one of LSR shown in Fig. 8.

7.2. Optimal values of f_B and $\hat{m}_b$ from MSR

Using a similar procedure as for the LSR, we study, in the case of MSR, the n-and t_c-stabilities of f_B and $\hat{m}_b$ for different values of the subtraction point μ. The analysis is illustrated in Fig. 13. The results are shown in Tables 4 and 5. One can notice that the sum rule does not stabilize for $\mu < 2$ GeV, while for other values of μ, the range of values t_c at which the n-stability is reached depends on the value of the subtraction point μ and are inside the range 32–42 GeV^2. We show the results in Table 4 an in Fig. 14 from which we deduce the result from the moments in units of MeV:

$$f_B|_{\rm MSR} = 203(11),$$
$$\hat{m}_b|_{\rm MSR} = 7460(164) \quad \Longrightarrow \quad \overline{m}_b(\overline{m}_b)|_{\rm MSR} = 4272(94). \tag{38}$$

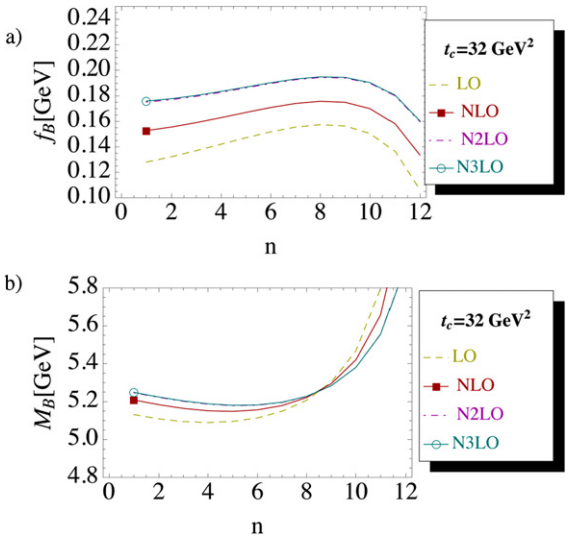

Fig. 12. (a) n-behavior of f_B from MSR for $t_c^B = 32$ GeV^2, for $\hat{m}_b = 7292$ MeV, for a given value of the subtraction point $\mu = 4$ GeV and for different truncations of the QCD PT series; (b) the same as (a) but for M_B.

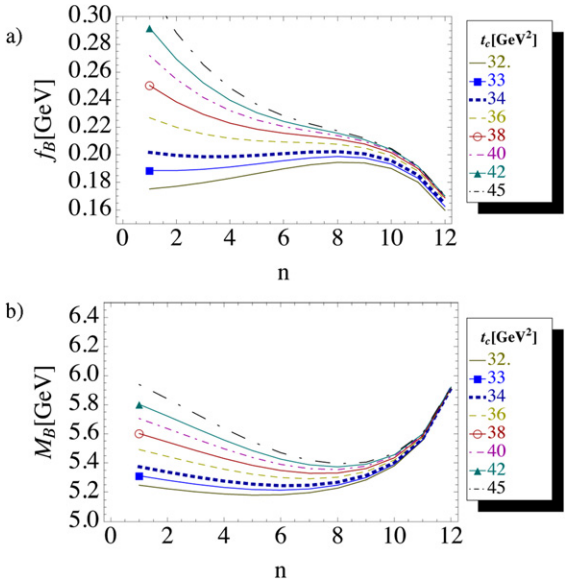

Fig. 13. (a) n behavior of f_B from MSR for different values of t_c, for $\hat{m}_b = 7292$ MeV and at the subtraction point $\mu = 4$ GeV; (b) the same as (a) but for M_B.

8. Final values of f_D, f_B and $\hat{m}_{c,b}$

As a final result of the present analysis, we take the average of the results from LSR for f_D and $\hat{m}_c$. This result is given in Eq. (30).

Table 5
Central values and corresponding errors for $\hat{m}_b$ in units of MeV from LSR and MSR at different values of the subtraction point μ in units of GeV. The + (resp. −) sign means that the values of $\hat{m}_b$ increase (resp. decrease) when the input increases (resp. decreases). The total error comes from a quadratic sum.

μ	$\hat{m}_b$	t_c	α_s	α_s^3	$\langle\bar{d}d\rangle$	$\langle G^2\rangle$	M_0^2	$\langle\bar{d}d\rangle^2$	$\langle G^3\rangle$	Total
LSR										
M_b	7586	−419	−95	−4	+7	+2	−26	0	0	431
MSR										
3	7188	−295	−110	−6	+6	+1	−174	+5	−0.5	360
4	7360	−301	−102	−6	+5	+1	−178	+4	−1	365
5	7490	−306	−99	−4	+8	+1	−179	+5	0	368
6	7598	−310	−99	−4	+9	+1	−179	+5	0	372
7	7686	−312	−97	−4	+9	+1	−180	+4	−1	374

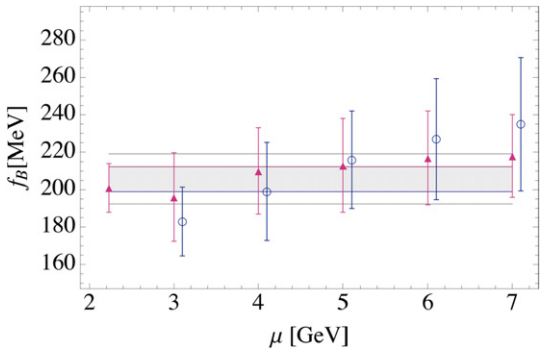

Fig. 14. Values of f_B from LSR (red triangle) and from MSR (blue open circle) at different values of the subtraction point μ and for $\hat{m}_b = 7292$ MeV. The filled (grey) region is the average with the corresponding averaged errors. The dashed horizontal lines are the values if one takes the errors from the best determination. (For interpretation of the references to color in this figure, the reader is referred to the web version of this Letter.)

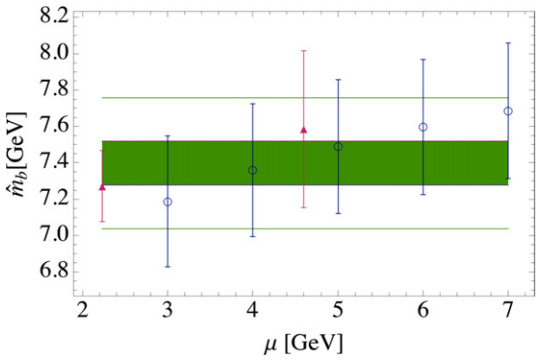

Fig. 15. Values of $\hat{m}_b$ from LSR (red triangle) and from MSR (blue open circle) at different values of the subtraction point μ. Same caption as in Fig. 14. (For interpretation of the references to color in this figure, the reader is referred to the web version of this Letter.)

The final results for f_B and $\hat{m}_b$ come from the average of the ones from LSR and MSR shown in Figs. 14 and 15, which are:

$$f_B = 206(7)\ \text{MeV} \equiv 1.58(5) f_\pi,$$

$$\hat{m}_b = 7398(121) \quad \Longrightarrow \quad \overline{m}_b(\overline{m}_b) = 4236(69)\ \text{MeV}, \tag{39}$$

where we have used the more precise value of $\overline{m}_b(\overline{m}_b)$ given in Table 1 for getting f_B. One can notice that $f_D \simeq f_B$, confirming previous results quoted in Eq. (4). This (almost) equality instead of the $1/\sqrt{m_b}$ behavior expected from HQET has been qualitatively interpreted in [60] using semi-local duality, while in [14] large mass corrections to the HQET lowest order expression have been found. These results are also confirmed by recent lattice calculations (see Table 8).

9. $SU(3)$ breaking and estimates of f_{D_s} and f_{B_s}

We extend the previous analysis for extracting f_{D_s,B_s} by including the m_s-corrections and by taking into account the $SU(3)$ breaking of the quark condensate $\langle\bar{s}s\rangle/\langle\bar{d}d\rangle$ given in Table 1.

9.1. f_{D_s} from LSR

In so doing, we use the complete PT expression in m_s of the QCD spectral function given to order α_s by [10]. The massless expressions for N2LO and N3LO have been used. The non-perturbative contributions come from the expressions given by [11, 18,26] where we have taken into account corrections of $\mathcal{O}(m_s^2)$ for the $d = 4$ condensates contributions while we have neglected the m_s corrections for the $d = 6$ condensates. We show in Fig. 16 the τ-behavior of f_{D_s} for different values of t_c at given $\mu = 1.4$ GeV. The results for different values of μ are given in Table 6 and Fig. 17.

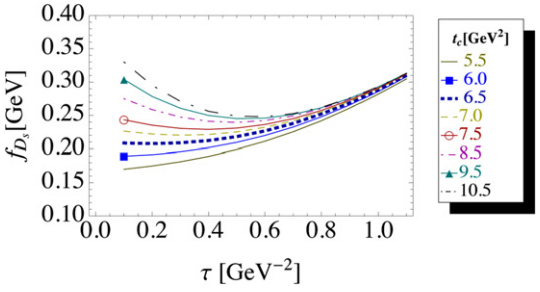

Fig. 16. τ-behavior of f_{D_s} from $\mathcal{L}_{\bar{d}c}$ for different values of t_c, for a given value of the subtraction point $\mu = 1.4$ GeV and for $\hat{m}_c = 1467$ MeV as given in Eq. (18).

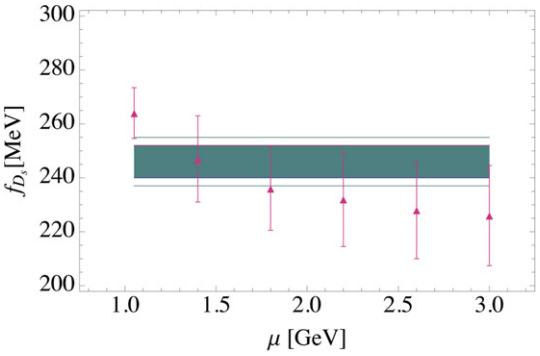

Fig. 17. Values of f_{D_s} from LSR at different values of the subtraction point μ and for $\hat{m}_c = 1467$ MeV. The filled (dark blue) region is the average with the corresponding averaged errors. The horizontal lines are the values if one takes the errors from the best determination. (For interpretation of the references to color in this figure, the reader is referred to the web version of this Letter.)

9.2. f_{B_s} from LSR and MSR

In this case, we only use the PT expression to order α_s of the QCD spectral function expanded up to order m_s^2 which is given by

Table 6
Central values and corresponding errors for f_{D_s} from the LSR at different values of the subtraction point μ and for $\hat{m}_c = 1467$ MeV. The + (resp. −) sign means that the values of f_P, $\hat{m}_c$ increase (resp. decrease) when the input increases (resp. decreases). The total error comes from a quadratic sum.

μ	f_{D_s}	t_c	α_s	α_s^3	m_c	$\langle\bar{d}d\rangle$	$\langle G^2\rangle$	M_0^2	m_s	$\langle\bar{s}s\rangle$	Total
$\tau^{-1/2}$	264	+8.2	+2.8	+3.2	+0.2	+0.8	+0.2	+0.3	+1.2	+0.5	9.4
1.4	247	+15	+1.0	+4.6	+0.4	+1.5	+0.7	+0.9	+1.7	+1.2	16
1.8	236	+15	+1.1	+3.3	+1.1	+1.0	+0.0	+0.3	+1.1	+0.5	15.5
2.2	232	+16.5	+1.2	+3.5	+1.1	+2.0	+1.4	+1.5	+2.2	+1.7	17.5
2.6	229	+17.6	+0.3	+1.8	+0.1	+1.2	+0.2	+0.5	+1.1	+0.7	18
3.0	226	+18.4	+1.2	+1.6	+0.2	+0.7	+0.1	+0.2	+1.0	+0.4	18.6

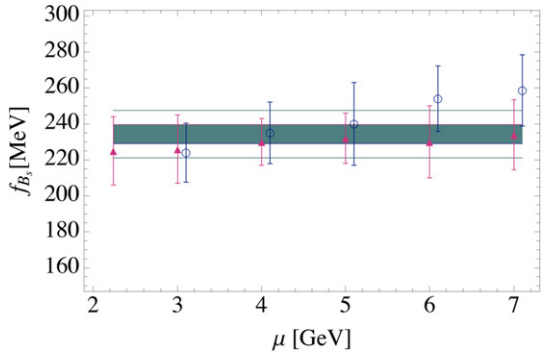

Fig. 18. Values of f_{B_s} from LSR (red triangle) and from MSR (blue open circle) at different values of the subtraction point μ and for $\hat{m}_b = 7292$ MeV. Same caption as in Fig. 17. (For interpretation of the references to color in this figure, the reader is referred to the web version of this Letter.)

[26]. The non-perturbative contributions are the same as in the case of f_{D_s}. We show in Fig. 19 the τ-behavior and n-behavior of f_{B_s} from LSR and MSR for different values of t_c at given $\mu = 4$ GeV. The results for different values of μ are given in Table 7 and Fig. 18.

9.3. Results for f_{D_s} and f_{B_s}

From the previous analysis, we deduce:

$$f_{D_s} = 246(6)\ \text{MeV} \equiv 1.59(5) f_K,$$
$$f_{B_s} = 234(5)\ \text{MeV} \equiv 1.51(4) f_K \tag{40}$$

which, with the help of the results in Eqs. (36) and (39) lead to:

$$\frac{f_{D_s}}{f_D} = 1.21(4), \qquad \frac{f_{B_s}}{f_B} = 1.14(3). \tag{41}$$

These results agree within the errors with the ones obtained by using the semi-analytic expressions of the correlator to order α_s [61]:

$$\frac{f_{D_s}}{f_D} = 1.15(4), \qquad \frac{f_{B_s}}{f_B} = 1.16(5), \tag{42}$$

with data when available [2,62] and with recent lattice simulations (see Table 8).

10. Rigorous model-independent upper bounds on $f_{D_{(s)},B_{(s)}}$

Upper bounds on f_D has been originally derived by NSV2Z [8] and improved four years later in [9–11] and more recently in [27].

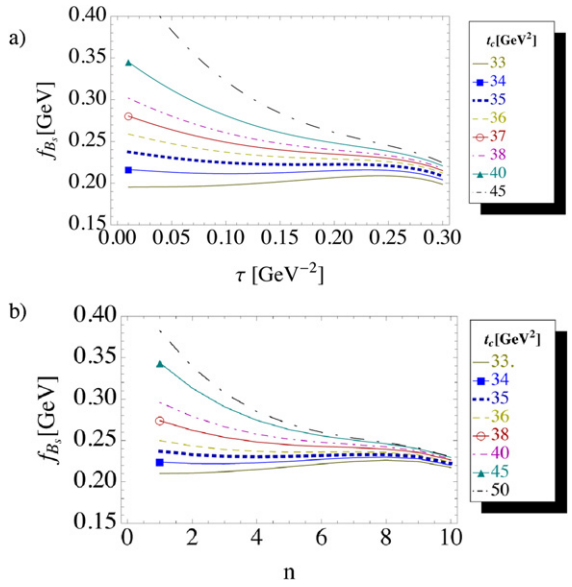

Fig. 19. (a) τ behavior of f_{B_s} from LSR for different values of t_c, for $\hat{m}_b = 7292$ MeV and at the subtraction point $\mu = 4$ GeV; (b) the same as (a) but n behavior of f_{B_s} from MSR.

In this Letter, we shall use LSR and the positivity of the continuum contributions to the spectral integral for obtaining the upper bounds on the decay constants. The procedure will be similar to the estimate done in previous sections where the optimal bound will be obtained at the minimum or inflexion point of the sum rules. In the D and D_s-meson channels, the LSR present a minimum which is well localized, while in the B and B_s channels, the LSR present instead an inflexion point which induces a new error for its localization, in addition to the errors induced by the QCD parameters which are the same as in the estimate of $f_{D,B}$ done in the previous sections. We show the results of the analysis for different values of the subtraction points in Fig. 20 from which we deduce the final results:

$$f_D \leqslant 218.4(1.4)\ \text{MeV} \equiv 1.68(1) f_\pi,$$
$$f_B \leqslant 235.3(3.8)\ \text{MeV} \equiv 1.80(3) f_\pi \tag{43}$$

and:

$$f_{D_s} \leqslant 253.7(1.5)\ \text{MeV} \equiv 1.61(1) f_K,$$
$$f_{B_s} \leqslant 251.3(5.5)\ \text{MeV} \equiv 1.61(4) f_K. \tag{44}$$

These bounds are stronger than earlier results in [9–11], while the results for f_{D,D_s} agree (within the large errors quoted there) with

Table 7
Central values and corresponding errors for f_B in units of MeV from the LSR and MSR at different values of the subtraction point μ in units of MeV for $\hat{m}_b = 7292$ MeV. The + (resp. −) sign means that the values of f_B increase (resp. decrease) when the input increases (resp. decreases). The total error comes from a quadratic sum.

μ	f_{B_s}	t_c	α_s	α_s^3	m_b	$\langle\bar{d}d\rangle$	$\langle G^2\rangle$	M_0^2	m_s	$\langle\bar{s}s\rangle$	Total
LSR											
$\tau^{-1/2}$	225	+18	−1.9	+3.5	−1.3	+1.4	+0.1	−0.4	+0.4	+0.7	19
3	226	+17	−8.5	+1.1	−1.3	+1.1	+0.0	−0.1	+0.5	+0.6	19
4	230	+10	−8	+0.8	−1.3	+1.1	+0.0	0.0	+0.5	+2.9	13
5	232	+11	−8.3	+0.7	−1.9	+1.2	−0.3	−0.5	+0.3	+2.5	14
6	230	+16	−10.9	+0.8	−0.9	+0.6	−0.2	−0.4	+0.4	+2.5	20
7	234	+16	−10.6	+0.7	−1.2	+1.2	+0.1	−0.3	+0.4	+2.7	20
MSR											
3	224	+8.0	−14	+0.4	−2.0	+1.4	−0.2	−1.1	+1.0	+1.0	16
4	235	+13	−10.6	+1.0	−2.1	+1.3	−0.1	−0.7	+1.0	+1.2	17
5	240	+12.4	−19.2	+1.1	−1.8	+1.2	0.0	−0.3	+1.1	+0.7	23
6	254	+12	−12.9	+1.0	−2.0	+2.3	−0.8	−2.4	+0.6	+1.5	18
7	258.6	+14	−13.2	+1.0	−2.4	+2.4	−0.5	−2.2	+0.7	+1.5	20

Table 8
Results from the open charm and beauty systems in units of MeV and comparison with experimental data and lattice simulations using $n_f = 2$ [63,64] and $n_f = 3$ [65,66] dynamical quarks. f_P are normalized as $f_\pi = 130.4$ MeV.

Charm	Bottom	Ref.
$\overline{m}_c(\overline{m}_c)$	$\overline{m}_b(\overline{m}_b)$	
1286(66)	4236(69)	This work
1280(40)	4290(140)	ETMC [63]
f_D	f_B	
$204(6) \equiv 1.56(5) f_\pi$	$206(7) \equiv 1.58(5) f_\pi$	This work
$\leqslant 218.4(1.4) \equiv 1.68(1) f_\pi$	$\leqslant 235.3(3.8) \equiv 1.80(3) f_\pi$	This work
207(9)	–	Data [2,62]
212(8)	195(12)	ETMC [63]
–	193(10)	ALPHA [64]
207(4)	190(13)	HPQCD [65]
219(11)	197(9)	FNAL [66]
f_{D_s}	f_{B_s}	
$246(6) \equiv 1.59(5) f_K$	$234(5) \equiv 1.51(4) f_\pi$	This work
$\leqslant 253.7(1.5) \equiv 1.61(1) f_K$	$\leqslant 251.3(5.5) \equiv 1.61(4) f_K$	This work
260(5.4)	–	Data [2,62]
248(6)	232(12)	ETMC [63]
–	219(12)	ALPHA [64]
248(2.5)	225(4)	HPQCD [65]
260(11)	242(10)	FNAL [66]

the ones in [27]. These large errors come mainly from m_c, μ and $\langle\bar{d}d\rangle$. The previous bounds can be used for excluding some experimental data and some theoretical estimates. In deriving these bounds, we have only used the positivity of the spectral function and we have checked that the SVZ-expansion converges quite well both for the PT radiative and non-perturbative corrections such that the approximate series is expected to reproduce with a good precision the exact solution. This fact can be (a posteriori) indicated by the remarkable agreement of our estimates with the lattice results. In this sense, we may state that the upper bound obtained previously is rigourous (at least within the SVZ framework).

11. Summary and conclusions

We have re-extracted the decay constants f_{D,D_s} and f_{B,B_s} and the running quark masses $\overline{m}_{c,b}(m_{c,b})$ using QCD spectral sum rules (QSSR). We have used as inputs, the recent values of the QCD (non-)perturbative parameters given in Table 1 and (for the first time) the renormalization group invariant quark and spontaneous masses in Eqs. (18) and (19). The results given in Eqs. (36), (39), (43) and (44) agree and improve existing QSSR results in the literature. Along the analysis, we have noticed that the values of the decay constants are very sensitive to the heavy quark mass and decrease when the heavy quark masses increase. Here we have used (for the first time) the scale-independent Renormalization Group Invariant (RGI) heavy quark masses in the analysis. We have translated the on-shell mass expressions of the PT spectral function known to N2LO into the $\overline{\rm MS}$ one where (as has been already noticed in previous works [19]) the PT series converge faster. We have also remarked that f_P and m_Q are affected by the choice of the continuum threshold t_c which gives the largest errors. Here, like in our previous works [13,14,19,25], we have taken the conservative range of t_c-values where the τ- or n-stability starts until the one where ones starts to have t_c-stability. We have also seen that the subtraction point μ affects the truncated results within the OPE which has been the sources of apparent discrepancies and large errors of the results in the literature. Here, we have considered carefully the results at each subtraction point and deduced, from these "QSSR data", the final results which should be independent on this arbitrary choice. In view of previous comments, we consider our results as improvements of the most recent ones to N2LO and using MDA in [25–27].

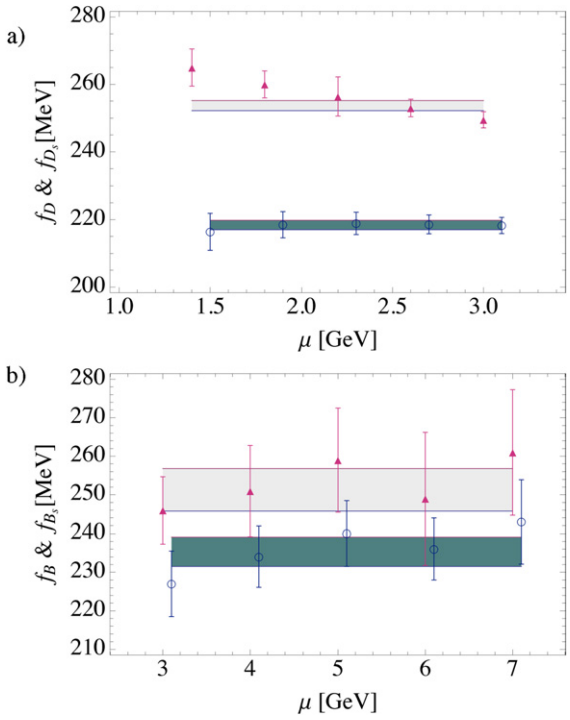

Fig. 20. (a) Upper bounds of f_{D_s} (red triangle) and of f_D (blue open circle) at different values of the subtraction point μ and for $\hat{m}_c = 1467$ MeV. The filled horizontal band is the average within the averaged error; (b) the same as a) but for f_{B_s} and f_B with $\hat{m}_b = 7292$ MeV. (For interpretation of the references to color in this figure, the reader is referred to the web version of this Letter.)

The results on f_D and f_{D_s} agree within the errors with the data compiled in [2,62], while the upper bound on f_{D_s} can already exclude some existing data and theoretical estimates.[12]

As one can see in Table 8, our results are comparable (in values and precisions) with recent lattice simulations including dynamical quarks [63–66].[13] These agreements are not surprising as both methods start from the same observables (the two-point correlator though evaluated in two different space–times) and use the 1st principles of QCD (here is the OPE in terms of the quarks and gluon condensates which semi-approximate the confinement regime). These agreements also confirm the accuracy of the MDA for describing the spectral function in the absence of a complete data, which has been tested earlier [5,6] and in this Letter from the charmonium and bottomium systems. MDA has been also successfully tested in the large N_c limit of QCD in [36].

References

[1] S. Narison, Talk given at the 16th International QCD Conference (QCD 12), Montpellier, 2–6 July 2012, arXiv:1209.2925 [hep-ph], 2012.
[2] Review by J. Rosner, S. Stone, in: J. Beringer et al. (Particle Data Group), Phys. Rev. D 86 (2012) 010001.
[3] M.A. Shifman, A.I. Vainshtein, V.I. Zakharov, Nucl. Phys. B 147 (1979) 385; M.A. Shifman, A.I Vainshtein, V.I. Zakharov, Nucl. Phys. B 147 (1979) 448.
[4] L.J. Reinders, H. Rubinstein, S. Yazaki, Phys. Rep. 127 (1985) 1.
[5] S. Narison, Cambridge Monogr. Part. Phys. Nucl. Phys. Cosmol. 17 (2002) 1, arXiv:hep-h/0205006.
[6] S. Narison, Lect. Notes Phys. 26 (1989) 1.
[7] S. Narison, Phys. Rep. 84 (1982) 263;

[12] Implications of the values of f_{D,D_s} on the determinations of the CKM mixing angles have been discussed in details in [67].
[13] A summary of the present results and comparisons with experiments and with the lattice ones will be presented elsewhere [1].

S. Narison, Acta Phys. Pol. B 26 (1995) 687;
S. Narison, arXiv:hep-ph/9510270.
[8] V.A. Novikov, et al., 8th Conf. Physics and Neutrino Astrophysics (Neutrinos 78), Purdue Univ., 28 April–2 May 1978.
[9] S. Narison, Z. Phys. C 14 (1982) 263.
[10] D.J. Broadhurst, S.C. Generalis, Open Univ. report, OUT-4102-8/R, 1982, unpublished.
[11] S.C. Generalis, PhD thesis, Open Univ. report, OUT-4102-13, 1982, unpublished.
[12] M.B. Voloshin, M.A. Shifman, Sov. J. Nucl. Phys. 45 (1987) 292;
H.D. Politzer, M.B. Wise, Phys. Lett. B 206 (1988) 504, 681.
[13] S. Narison, Phys. Lett. B 198 (1987) 104;
S. Narison, Phys. Lett. B 285 (1982) 141.
[14] S. Narison, Phys. Lett. B 279 (1992) 137;
S. Narison, Phys. Lett. B 308 (1993) 365;
S. Narison, Z. Phys. C 55 (1992) 671.
[15] G. Alexandrou, et al., Phys. Lett. B 256 (1991) 60, CERN-TH 6113, 1992;
C. Allton, et al., Nucl. Phys. B 349 (1991) 598;
M. Lusignoli, et al., Rome preprint 792, 1991;
C. Bernard, et al., Lattice workshop, Tallahassee, 1990.
[16] D.J. Broadhurst, Phys. Lett. B 101 (1981) 423, and private communication.
[17] K.G. Chetyrkin, M. Steinhauser, Phys. Lett. B 502 (2001) 104;
K.G. Chetyrkin, M. Steinhauser, arXiv:hep-ph/0108017.
[18] M. Jamin, M. Münz, Z. Phys. C 60 (1993) 569.
[19] S. Narison, Phys. Lett. B 341 (1994) 73;
S. Narison, Nucl. Phys. B (Proc. Suppl.) 74 (1999) 304.
[20] R. Tarrach, Nucl. Phys. B 183 (1981) 384.
[21] R. Coquereaux, Annals of Physics 125 (1980) 401;
P. Binetruy, T. Sücker, Nucl. Phys. B 178 (1981) 293.
[22] S. Narison, Phys. Lett. B 197 (1987) 405;
S. Narison, Phys. Lett. B 216 (1989) 191.
[23] N. Gray, D.J. Broadhurst, W. Grafe, K. Schilcher, Z. Phys. C 48 (1990) 673;
J. Fleischer, F. Jegerlehner, O.V. Tarasov, O.L. Veretin, Nucl. Phys. B 539 (1999) 671.
[24] K.G. Chetyrkin, M. Steinhauser, Nucl. Phys. B 573 (2000) 617;
K. Melnikov, T. van Ritbergen, arXiv:hep-ph/9912391.
[25] S. Narison, Phys. Lett. B 520 (2001) 115.
[26] M. Jamin, B.O. Lange, Phys. Rev. D 65 (2002) 056005.
[27] A. Khodjamirian, Phys. Rev. D 79 (2009) 031503.
[28] A. Penin, M. Steinhauser, Phys. Rev. D 65 (2002) 054006.
[29] D.J. Broadhurst, M. Grozin, Phys. Lett. B 274 (1992) 421;
E. Bagan, P. Ball, V. Braun, H.G. Dosch, Phys. Lett. B 278 (1992) 457;
M. Neubert, Phys. Rev. D 45 (1992) 2451;
V. Eletsky, A.V. Shuryak, Phys. Lett. B 276 (1993) 365.
[30] S. Narison, V.I. Zakharov, Phys. Lett. B 679 (2009) 355.
[31] K.G. Chetyrkin, S. Narison, V.I. Zakharov, Nucl. Phys. B 550 (1999) 353;
S. Narison, V.I. Zakharov, Phys. Lett. B 522 (2001) 266.
[32] For reviews, see e.g. V.I. Zakharov, Nucl. Phys. B (Proc. Suppl.) 164 (2007) 240;
S. Narison, Nucl. Phys. B (Proc. Suppl.) 164 (2007) 225.
[33] E.G. Floratos, S. Narison, E. de Rafael, Nucl. Phys. B 155 (1979) 155.
[34] S. Narison, E. de Rafael, Phys. Lett. B 103 (1981) 57.
[35] S. Narison, Phys. Lett. B 693 (2010) 559;
S. Narison, Phys. Lett. B 705 (2011) 544;
S. Narison, Phys. Lett. B 706 (2011) 412;
S. Narison, Phys. Lett. B 707 (2012) 259.
[36] E. de Rafael, Nucl. Phys. B (Proc. Suppl.) 96 (2001) 316;
S. Peris, B. Phily, E. de Rafael, Phys. Rev. Lett. 86 (2001) 14.
[37] J.S. Bell, R.A. Bertlmann, Nucl. Phys. B 227 (1983) 435;
R.A. Bertlmann, Acta Phys. Austriaca 53 (1981) 305;
R.A. Bertlmann, H. Neufeld, Z. Phys. C 27 (1985) 437.
[38] K.G. Chetyrkin, J.H. Kühn, M. Steinhauser, arXiv:hep-ph/0004189, and references therein.
[39] S. Narison, Phys. Lett. B 673 (2009) 30.
[40] E. Braaten, S. Narison, A. Pich, Nucl. Phys. B 373 (1992) 581;
S. Narison, A. Pich, Phys. Lett. B 211 (1988) 183.
[41] For a recent review, see e.g. S. Bethke, Talk given at the 16th International QCD Conference (QCD 12), Montpellier, 2–6 July 2012, arXiv:1210.0325 [hep-ex].
[42] K. Nakamura, et al., PDG Collaboration, J. Phys. G 37 (2010) 075021.
[43] S. Narison, Phys. Rev. D 74 (2006) 034013.
[44] S. Narison, arXiv:hep-ph/0202200;
S. Narison, Nucl. Phys. B (Proc. Suppl.) 86 (2000) 242;
S. Narison, Phys. Lett. B 216 (1989) 191;
S. Narison, Phys. Lett. B 358 (1995) 113;
S. Narison, Phys. Lett. B 466 (1999) 345;
S. Narison, Riv. Nuov. Cim. 10 (2) (1987) 1;
S. Narison, H.G. Dosch, Phys. Lett. B 417 (1998) 173;
S. Narison, N. Paver, E. de Rafael, D. Treleani, Nucl. Phys. B 212 (1983) 365;
S. Narison, E. de Rafael, Phys. Lett. B 103 (1981) 57;
C. Becchi, S. Narison, E. de Rafael, F.J. Yndurain, Z. Phys. C 8 (1981) 335.
[45] S. Narison, Phys. Lett. B 197 (1987) 405;
S. Narison, Phys. Lett. B 341 (1994) 73;
S. Narison, Phys. Lett. B 520 (2001) 115.
[46] B.L. Ioffe, K.N. Zyablyuk, Eur. Phys. J. C 27 (2003) 229;
B.L. Ioffe, Prog. Part. Nucl. Phys. 56 (2006) 232.
[47] R.A. Albuquerque, S. Narison, M. Nielsen, Phys. Lett. B 684 (2010) 236.
[48] Y. Chung, et al., Z. Phys. C 25 (1984) 151;
H.G. Dosch, Non-Perturbative Methods, Montpellier, 1985;
H.G. Dosch, M. Jamin, S. Narison, Phys. Lett. B 220 (1989) 251.
[49] B.L. Ioffe, Nucl. Phys. B 188 (1981) 317;
B.L. Ioffe, Nucl. Phys. B 191 (1981) 591;
A.A. Ovchinnikov, A.A. Pivovarov, Yad. Fiz. 48 (1988) 1135.
[50] S. Narison, Phys. Lett. B 605 (2005) 319.
[51] G. Launer, S. Narison, R. Tarrach, Z. Phys. C 26 (1984) 433.
[52] S. Narison, Phys. Lett. B 300 (1993) 293;
S. Narison, Phys. Lett. B 361 (1995) 121.
[53] R.A. Bertlmann, G. Launer, E. de Rafael, Nucl. Phys. B 250 (1985) 61;
R.A. Bertlmann, et al., Z. Phys. C 39 (1988) 231.
[54] F.J. Yndurain, arXiv:hep-ph/9903457.
[55] S. Narison, Phys. Lett. B 387 (1996) 162.
[56] S. Narison, Phys. Lett. B 361 (1995) 121;
S. Narison, Phys. Lett. B 624 (2005) 223.
[57] For reviews, see e.g. F.S. Navarra, M. Nielsen, S.H. Lee, Phys. Rep. 497 (2010) 41;
S.L. Zhu, Int. J. Mod. Phys. E 17 (2008) 283.
[58] D. Harnett, R.T. Kleiv, T.G. Steele, H.-y. Jin, arXiv:1206.6776 [hep-ph];
D. Harnett, R.T. Kleiv, T.G. Steele, H.-y. Jin, arXiv:1208.3273 [hep-ph];
R. Berg, D. Harnett, R.T. Kleiv, T.G. Steele, Phys. Rev. D 86 (2012) 034002;
R. Berg, D. Harnett, R.T. Kleiv, T.G. Steele, H.-y. Jin, arXiv:1209.4102 [hep-ph].
[59] R.M. Albuquerque, F. Fanomezana, S. Narison, A. Rabemananjara, Phys. Lett. B 715 (2012) 129;
R.M. Albuquerque, F. Fanomezana, S. Narison, A. Rabemananjara, arXiv:1210.2990 [hep-ph];
R.D. Matheus, S. Narison, M. Nielsen, J.M. Richard, Phys. Rev. D 75 (2007) 014005.
[60] S. Narison, K. Zalewski, Phys. Lett. B 320 (1994) 369.
[61] S. Narison, Phys. Lett. B 322 (1994) 247.
[62] D. Asner, et al., arXiv:1010.1589 [hep-ex], http://www.slac.stanford.edu/xorg/hfag/charm/.
[63] ETM collaboration, P. Dimopoulos, et al., JHEP 1201 (2012) 046;
N. Carrasco, A. Shindler, Lattice 2012, and private communication from G. Rossi.
[64] ALPHA Collaboration, J. Heitger, Talk given at the 16th International QCD Conference (QCD 12), Montpellier, 2–6th July 2012.
[65] HPQCD Collaboration, arXiv:1008.4018 [hep-lat].
[66] A. Bazavov, et al., arXiv:1112.3051 [hep-lat].
[67] S. Narison, Phys. Lett. B 668 (2008) 308.